

Modeling the effects of irrigation on land surface fluxes and states over the conterminous United States: Sensitivity to input data and model parameters

Guoyong Leng,^{1,2,3} Maoyi Huang,² Qihong Tang,¹ William J. Sacks,⁴ Huimin Lei,^{2,5} and L. Ruby Leung²

Received 20 February 2013; revised 13 August 2013; accepted 25 August 2013.

[1] Previous studies on irrigation impacts on land surface fluxes/states were mainly conducted as sensitivity experiments, with limited analysis of uncertainties from the input data and model irrigation schemes used. In this study, we calibrated and evaluated the performance of irrigation water use simulated by the Community Land Model version 4 (CLM4) against observations from agriculture census. We investigated the impacts of irrigation on land surface fluxes and states over the conterminous United States (CONUS) and explored possible directions of improvement. Specifically, we found large uncertainty in the irrigation area data from two widely used sources and CLM4 tended to produce unrealistically large temporal variations of irrigation demand for applications at the water resources region scale over CONUS. At seasonal to interannual time scales, the effects of irrigation on surface energy partitioning appeared to be large and persistent, and more pronounced in dry than wet years. Even with model calibration to yield overall good agreement with the irrigation amounts from the National Agricultural Statistics Service, differences between the two irrigation area data sets still dominate the differences in the interannual variability of land surface responses to irrigation. Our results suggest that irrigation amount simulated by CLM4 can be improved by calibrating model parameter values and accurate representation of the spatial distribution and intensity of irrigated areas. Furthermore, through a set of numerical experiments, the deficiency in the current parameterization is evaluated and a critical path forward to a realistic assessment of irrigation impacts using an earth system modeling approach is recommended.

Citation: Leng, G., M. Huang, Q. Tang, W. J. Sacks, H. Lei, and L. R. Leung (2013), Modeling the effects of irrigation on land surface fluxes and states over the conterminous United States: Sensitivity to input data and model parameters, *J. Geophys. Res. Atmos.*, 118, doi:10.1002/jgrd.50792.

1. Introduction

[2] Humans are affecting the regional climate not only by changing land cover but also through changes in land management practice. In hot and dry regions, irrigation practice increases the amount of water available for plants, releasing more water into the air through evapotranspiration [Boucher *et al.*, 2004]. Globally, the increase in water vapor flows from

land ($2600 \text{ km}^3 \text{ yr}^{-1}$) caused by irrigation is in the same order of magnitude as the decrease ($3600 \text{ km}^3 \text{ yr}^{-1}$) induced by deforestation [Gordon *et al.*, 2005]. Thus, irrigated agriculture management practices can have substantial impact on regional/local climate and land surface hydrology [Pielke *et al.*, 2007; Sacks *et al.*, 2009]. Over the past 200 years, the global irrigated area has increased from 8×10^6 ha around the year 1800 to 2.52×10^8 ha around the year 2000 [Thenkabail *et al.*, 2009]. World agriculture has consumed about 87% of global fresh water withdrawal by humans [Douglas *et al.*, 2009] and significantly disturbed the hydrological cycle [Kustu *et al.*, 2010]. Understanding the impact of irrigation on land surface fluxes/states and their interactions with atmospheric processes is crucial for understanding historical climate change and modeling future climate at local and regional scales [Bonfils and Lobell, 2007; Diffenbaugh, 2009].

[3] The impacts of irrigation on land surface water budget and energy fluxes have received a lot of attentions in recent years. Many studies have used land surface model uncoupled [Douglas *et al.*, 2006; Haddeland *et al.*, 2006; Biggs *et al.*, 2008] or coupled [Adegoke *et al.*, 2003; Douglas *et al.*, 2009; Kueppers *et al.*, 2007; Saeed *et al.*, 2009] with regional

Additional supporting information may be found in the online version of this article.

¹Institute of Geographic Sciences and Natural Resources Research, Chinese Academy of Sciences, Beijing, China.

²Atmospheric Sciences and Global Change Division, Pacific Northwest National Laboratory, Richland, Washington, USA.

³University of Chinese Academy of Sciences, Beijing, China.

⁴National Center for Atmospheric Research, Boulder, Colorado, USA.

⁵Department of Hydraulic Engineering, Tsinghua University, Beijing, China.

Corresponding author: M. Huang, Pacific Northwest National Laboratory, PO Box 999, Richland, WA 99352, USA. (maoyi.huang@pnl.gov)

©2013. American Geophysical Union. All Rights Reserved.
2169-897X/13/10.1002/jgrd.50792

atmospheric model. The uncoupled model (i.e., offline) simulations show that irrigation generally leads to decrease in runoff [Haddeland *et al.*, 2006; Tang *et al.*, 2007], increase in latent heat flux, decrease in sensible heat flux, and consequently cooling of the land surface [Shibuo *et al.*, 2007; Tang *et al.*, 2007]. In some areas with extensive irrigation, the cooling effect by irrigation can match or even exceed the impacts of greenhouse warming [Diffenbaugh, 2009; Kueppers *et al.*, 2007; Lobell *et al.*, 2008; Puma and Cook, 2010]. The irrigation effects could potentially enhance shallow and deep convections and increase cloud formation [Kawase *et al.*, 2008; Qian *et al.*, 2013] and precipitation [DeAngelis *et al.*, 2010; Koster *et al.*, 2004; Segal *et al.*, 1998] by modifying the depths of planetary boundary layer, lifting condensation level, and mixing layer. Irrigation practice over a large area may even alter the large-scale circulations and therefore have broader implications for human society [Douglas *et al.*, 2009; Lee *et al.*, 2009; Saeed *et al.*, 2009]. Although irrigation cooling effect is estimated to be negligible for global average near-surface temperature, irrigation has significantly altered regional and local climate in many northern midlatitude regions such as the central and southeastern United States, southern and Southeast Asia, and the agricultural regions of southeastern China [Sacks *et al.*, 2009]. Irrigation impacts are likely to increase in the context of a rapid increase of global food demand [Tilman *et al.*, 2011] and a growing world population that is expected to reach about 9 billion by middle of the century [van Vuuren *et al.*, 2012] in the Shared Socioeconomic Pathways for the Intergovernmental Panel on Climate Change fifth Assessment Report on climate change.

[4] As previous modeling studies focused mostly on the potential effects of irrigation, limited studies reported the irrigation volume and area simulated by the models [Haddeland *et al.*, 2006; Hanasaki *et al.*, 2006; Tang *et al.*, 2007]. Due to differences in model physics and irrigation scheme, the magnitude and spatial pattern of irrigation volume simulated by the models can differ rather substantially [Sacks *et al.*, 2009; Sorooshian *et al.*, 2012] and may potentially influence the simulated effects of irrigation on land surface water budget and energy fluxes and regional/local climate. The question of how much water should be added into the soil columns to mimic irrigation has been assessed recently mainly through sensitivity studies [Kanamaru and Kanamitsu, 2008; Kueppers and Snyder, 2011; Lobell *et al.*, 2009]. Kueppers *et al.* [2008] found that the simulated effects of irrigation were model dependent, with even sign change for daily minimum temperature. More specifically, the modeled effects of irrigation are complicated by both the area and volume of irrigation [Ozdogan *et al.*, 2010]. Model parameter and input data uncertainties combined could also lead to uncertain predictions, resulting in ambiguous representation of controlling processes [Franks *et al.*, 1997] in irrigation modeling studies.

[5] This study aims to evaluate and improve the irrigation simulations from CLM4 driven by observed atmospheric conditions using statistics from census. More specifically, we assess the performance of the irrigation scheme in CLM4 using different prescribed irrigated area maps and calibrate the related model parameters using observational irrigation water amount from agricultural census. With the calibrated irrigation scheme, this study also investigates the

impacts of irrigation on land surface fluxes and states over the conterminous United States. This paper is organized as follows: Section 2 includes a brief description of CLM4, experimental design, and data. Section 3 presents the model performance to the prescribed irrigated area maps and model parameters. It demonstrates the irrigation impacts on surface heating fluxes and runoff and shows the potential of improving the irrigation representations in CLM by constraining water availability. Conclusion and Discussion are summarized in section 4.

2. Data and Methodology

2.1. Data

[6] Accurate geospatial information on the extent of irrigated area is fundamental and crucial to many aspects of Earth systems science and global change studies, including interactions between the land surface and atmosphere [Ozdogan and Gutman, 2008]. In recent years, several studies have addressed the challenges of irrigation extent mapping using census data or by remote-sensing techniques for classification of potential irrigation. Siebert *et al.* [2005] provided a Global Map of Irrigated Area (GMIA) representing the fraction of area equipped for irrigation around the year of 2000 with a spatial resolution of 5 arc minutes (hereafter denoted as F_{GMIA}). They combined input data sets from various sources such as The Food and Agriculture Organization of the United Nations reports, the United Nations, Ministries of Agriculture and land use, and land cover data set from United States Geological Survey (USGS) for the year 2000. This map has been widely used in modeling [Sacks *et al.*, 2009; Saeed *et al.*, 2009] and observational studies [Bonfils and Lobell, 2007; Zhu *et al.*, 2012] and has become the de facto information source for spatial distribution of global irrigated areas of the present day.

[7] Ozdogan and Gutman [2008] produced a high-resolution (~500 m) irrigated area map (hereafter denoted as F_{MODIS}) for the continental United States using a remote-sensing approach. They combined the Nadir Bidirectional Distribution Function Adjusted Reflectance (NBAR) data acquired during 2001, gridded climate-based indices of surface moisture status and a map of cultivated areas as inputs to their data set. This new map provides a reasonably accurate spatial distribution of irrigation extent circa 2001, which has been comprehensively validated against agricultural statistics (i.e., The National Agricultural Statistics Service reports for the year 2002) at the state and county level. The new map, provided in terms of percentage of potential irrigation area in each grid cell, has been used in land surface modeling studies [Ozdogan *et al.*, 2010] and climate modeling studies [Qian *et al.*, 2013].

[8] Conducted every 5 years, the U.S. Department of Agriculture's (USDA) Agricultural Statistics Service (NASS) reports comprehensive agricultural data collected from every state and county in the nation and is the leading source of facts and figures of U.S. farms. This data set provides the detailed information on U.S. farms and ranches, including the acres irrigated and acre-feet water withdrawal for irrigation through sampling of existing farms, and is the only source of comprehensive agricultural data at the state and county level in the United States. We collected the gross irrigation withdrawal data from Census of Agriculture (<http://>

www.nass.usda.gov/Census_of_Agriculture/) for 1987, 1992, 1997, 2002, and 2007 for each Water Resources Region (see definition of the Water Resources Regions in Figure S1 in the supporting information) over CONUS for evaluation of the irrigation water demand simulated by the model.

[9] As modeling of irrigation water demand is (among other things) directly related to the geospatial information on irrigated cropland, it is expected that errors from the irrigation extent map may influence the irrigation water demand estimates. This is especially true for those regions with large discrepancy among different irrigated fraction data sets. Hence, both gridded data sets were mapped to 0.125° resolution as inputs to CLM4 to investigate the characteristics of different irrigation maps on simulated land surface fluxes and state. We also aggregated the two irrigation fraction data sets to water resources region level and compared them with the 2002 USDA (U.S. Department of Agriculture) Census of Agriculture (hereafter denoted as NASS₂₀₀₂) to quantify the uncertainties from irrigation map. The 0.05° resolution actual evapotranspiration based entirely on satellite data was obtained from Tang *et al.* [2009a, 2009b] and aggregated at each water resources region for evaluating the CLM4-simulated evapotranspiration fluxes. The satellite-based evapotranspiration product is generated using a remote-sensing approach that works best over areas where there is substantial diversity in vegetation types within the remote-sensing window. The contrast in vegetation between irrigated and adjacent nonirrigated areas meets the diversity requirements well. The satellite-based evapotranspiration product has been used in irrigation impact assessments in western United States [Anderson *et al.*, 2012; Famiglietti *et al.*, 2011; Sorooshian *et al.*, 2012; Tang *et al.*, 2009a, 2009b] and hydrological applications [Cheng *et al.*, 2011; Gao *et al.*, 2010; Tang *et al.*, 2010].

2.2. Methodology

2.2.1. Model Description and Configurations

[10] The Community Land Model version 4.0 (CLM4) is the land surface model used in this study. CLM4 represents extensive modifications in its model structure and parameterizations over previous CLM versions, including enhancements in the representations of hydrological processes such as runoff generation, groundwater dynamics, soil hydrology, snow module, and surface albedo [Lawrence *et al.*, 2011a, 2011b]. Used alone and in the Community Earth System Model (CESM) [Collins *et al.*, 2006; Gent *et al.*, 2010; Lawrence *et al.*, 2011a, 2011b], CLM4 has been designed and used for studies of interannual and interdecadal variability, paleoclimate regimes, and projections of future changes of the global climate system [Gent *et al.*, 2010; Lawrence *et al.*, 2011a, 2011b]. Driven by observed phenology from satellite (hereafter denoted as CLM4-SP), CLM4 could also be used as a traditional land surface model to simulate water and energy fluxes and state variables. In this study, CLM4-SP was applied to simulate irrigation and land surface water and energy budgets.

[11] An irrigation scheme was integrated into CLM4 to irrigate cropland areas that are equipped for irrigation. The irrigation scheme is described in the CESM1.0 technical note at <http://www.cesm.ucar.edu/models/cesm1.0/clm/CLMcropANDirrigTechDescriptions.pdf> and summarized here. In CLM4, irrigation is implemented for the C3 generic

crop only and responds dynamically to climate. When irrigation is enabled, the cropland area of each grid cell is divided into irrigated and nonirrigated fractions according to a data set of areas equipped for irrigation [Siebert *et al.*, 2005]. The area of irrigated cropland in each grid cell is given by the smaller of (1) the grid cell's total cropland area and (2) the grid cell's area equipped for irrigation. Any remaining cropland area in the grid cell is then assigned to nonirrigated cropland. Irrigated and nonirrigated crops are placed on separate soil columns, so that irrigation is only applied to the soil beneath the irrigated crops. In irrigated croplands, a check is made once per day to determine whether irrigation is required on that day. This check is made in the first time step after 6 A.M. local time. Irrigation is required if (1) the crop leaf area > 0 and (2) $\beta_i < 1$, i.e., water is limiting photosynthesis. β_i is a function that decreases the carboxylation rate through changes in soil water and varies between 0 and 1, corresponding to when the soil is dry or when the soil is wet.

[12] If irrigation is required, the model computes the deficit between the current soil moisture content and the target soil moisture content; this deficit is the amount of water that will be added through irrigation. The target soil moisture content in each soil layer i ($W_{\text{target},i}$, kg m^{-2}) is a weighted average of (1) the minimum soil moisture content that results in no water stress in that layer ($W_{o,i}$, kg m^{-2}) and (2) the soil moisture content at saturation in that layer ($W_{\text{sat},i}$, kg m^{-2}):

$$W_{\text{target},i} = (1 - F_{\text{irrig}}) \times W_{o,i} + F_{\text{irrig}} \times W_{\text{sat},i} \quad (1)$$

[13] $W_{o,i}$ is determined by inverting equation (2) to solve for the value of S_i (soil wetness) that makes $\Psi_i = \Psi_o$ (where Ψ_i is the soil water matric potential and Ψ_o is the soil water potential when the stomata are fully open), and then converting this value to units of kg m^{-2} . $W_{\text{sat},i}$ is calculated simply by converting the effective porosity [see Oleson *et al.*, 2010, section 7.2] to units of kg m^{-2} .

$$\psi_i = \psi_{\text{sat},i} S_i^{-B_i} \geq \psi_c \quad (2)$$

where Ψ_i is the soil water matric potential (mm) and Ψ_c is the soil water matric potential (mm) when the stomata are fully closed. Ψ_{sat} and B_i are the saturated soil matric potential (mm) and the Clapp and Hornberger [1978] parameter, respectively.

[14] F_{irrig} is a weighted factor between 0 and 1, corresponding to setting the soil moisture target just enough to prevent plant water stress for crops or to full soil saturation. The default weighted factor value (i.e., $F_{\text{irrig}} = 0.7$) was determined empirically so that the global, annual irrigation amounts approximately match the observed gross irrigation water use near year 2000 (i.e., total water withdrawals for irrigation: $\sim 2500\text{--}3000 \text{ km}^3 \text{ year}^{-1}$ [Shiklomanov, 2000]). The total water deficit (W_{deficit} , kg m^{-2}) of the column is then determined by

$$W_{\text{deficit}} = \sum_i \max(W_{\text{target},i} - W_{\text{liq},i}, 0) \quad (3)$$

where $W_{\text{liq},i}$ (kg m^{-2}) is the current soil water content of layer i . The max function ensures that a surplus in any layer cannot reduce the deficit in other layers. The sum is taken only over soil layers that contain roots. In addition, if the temperature of

Table 1. Description of Numerical Experiments

Name	Irrigation	Weighted Factor (F_{irrig})	Irrigated Fraction Map	Constrained by Total Runoff	Simulation Period
CLM _{noirrig}	No	—	—	—	1979–2007
CLM _{GMA, nocal}	Yes	Default	F _{GMA}	No	1979–2007
CLM _{MODIS, nocal}	Yes	Default	F _{MODIS}	No	1979–2007
CLM _{GMA, cal}	Yes	Calibrated	F _{GMA}	No	1979–2007
CLM _{MODIS, cal}	Yes	Calibrated	F _{MODIS}	No	1979–2007
CLM _{GMA, con}	Yes	Calibrated	F _{GMA}	Yes	2007
CLM _{MODIS, con}	Yes	Calibrated	F _{MODIS}	Yes	2007

any soil layer is below freezing, then the sum only includes layers above the topmost frozen soil layer.

[15] The amount of water added to this column through irrigation is then equal to W_{deficit} . This irrigation is applied at a constant rate over 4 hours after 6 A.M. Irrigation water is applied directly to the ground surface, bypassing canopy interception, which would mimic a drip irrigation system. The irrigation amount is removed from the total liquid runoff to simulate the removal from local rivers within each grid cell. We note that the CLM4 irrigation scheme used in this study, as well as models used in many other previous studies [e.g., *Kueppers et al.*, 2007; *Lobell et al.*, 2008; *Sacks et al.*, 2009; *Ozdogan et al.*, 2010; *Sorooshian et al.*, 2011], does not explicitly account for irrigation fed by groundwater. Although groundwater is an important source of irrigation water in some regions, this study focuses only on irrigation using surface water and its effects on surface fluxes. The implementation and application of a groundwater pumping scheme is addressed in a follow-up study [*Leng et al.*, 2013] that aims to evaluate the effects of groundwater-fed irrigation on terrestrial hydrology over the conterminous United States.

[16] High-quality atmospheric forcing data sets are critical for modeling studies. This study uses the assimilated forcing data sets derived by the multi-institutional North American Land Data Assimilation System (NLDAS) project [*Cosgrove et al.*, 2003]. These comprehensive forcing data sets include precipitation, shortwave and longwave radiation, air temperature, humidity, and wind speed, which are available at 0.125 grid resolutions hourly across the conterminous United States (details given by *Cosgrove et al.* [2003]). Precipitation data were produced by combining observations from field stations, level 4 precipitation retrievals from Next Generation Weather Radar systems and satellites, and are well suited for hydrologic studies. The NLDAS phase II (i.e., NLDAS-2) meteorological field [*Xia et al.*, 2012] is used to force CLM4 at an hourly time step from 1979–2007. Soil, vegetation, and land cover characteristics of the grid cells were derived from the 0.05° CLM input data set developed by *Ke et al.* [2012].

2.2.2. Experimental Design

[17] Numerical experiments described below are summarized in Table 1. A default simulation without irrigation (hereafter denoted CLM_{noirrig}) was conducted in offline mode from 1979–2007, using the initial condition generated by recycling the NLDAS2 forcing in 1979–2007 for 36 cycles (i.e., ~1000 years) until all state variables in CLM4, including soil moisture, temperature, and groundwater table depth, reached equilibrium. Additionally, four 29 year offline simulations were performed from 1979–2007 as sensitivity experiments. All the 29 year simulations started from a common initial condition as used in the default simulation.

The first two simulations included irrigation (hereafter denoted CLM_{GMA,nocal} and CLM_{MODIS,nocal}), which used irrigation fraction data from F_{GMA} and F_{MODIS}, respectively with $F_{\text{irrig}} = 0.7$, the default single value for each grid cell in CLM4. The difference between these two runs with irrigation and the default run (i.e., CLM_{noirrig}) provided an estimate of the response of land surface fluxes and states to irrigation, while the difference between the two runs with irrigation provides a comparison of characteristics using different irrigation fraction data. We then calibrated F_{irrig} by perturbing it between (0, 1) at a regular interval of 0.05 using F_{GMA} and F_{MODIS} as inputs, respectively, and by comparing the simulated irrigation amounts with the NASS₂₀₀₂ census data to select the best parameter value for each water resources region. Each grid cell was then assigned the calibrated F_{irrig} value in order to capture the realistic irrigation amount at the water resources region scale. Two additional experiments, denoted as CLM_{GMA,cal} and CLM_{MODIS,cal}, respectively, were then conducted with the new set of calibrated parameters for each simulation using F_{GMA} and F_{MODIS} as the irrigation fraction data.

[18] To illustrate the importance of interannual variability of land surface variables to irrigation, we selected a relatively wet year, 1997 and a relatively dry year, 2007 from the 29 year simulation results after calibration (i.e., CLM_{GMA,cal} and CLM_{MODIS,cal}) based on the Palmer Drought Severity Index data [*Dai*, 2011] to focus our analysis. All times are given in Coordinated Universal Time (UTC). The last two 1 year (i.e., 2007) experiments (i.e., CLM_{GMA,con} and CLM_{MODIS,con}) were performed to examine the effects of constraints from local water availability for irrigation. That is, the actual irrigation amount is the minimum of the irrigation demands and total runoff (Q_{runoff}) at each time step, different from the standard assumption in the irrigation scheme in CLM4 that water is always available to meet irrigation demands, as true in other irrigation simulations in this paper (i.e., CLM_{GMA,nocal}, CLM_{MODIS,nocal}, CLM_{GMA,cal}, and CLM_{MODIS,cal}) and previous modeling studies [e.g., *Sacks et al.*, 2009; *Ozdogan et al.*, 2010]. This represents the opposite extreme from unlimited water supply in that we assume that water for irrigation can only come from local water availability, while in reality, water can come from water storage such as rivers and reservoirs. We used the dry year 2007 to investigate the characteristics of irrigation influence on land surface fluxes and states after accounting for the constraints of water availability. In the following analyses, we focus on six water resources regions (i.e., Lower Mississippi, Missouri, Texas Gulf, Upper Colorado, Pacific Northwest, and California in Figure S1) with the highest irrigation rates, where we expect the direct irrigation effects to be the strongest.

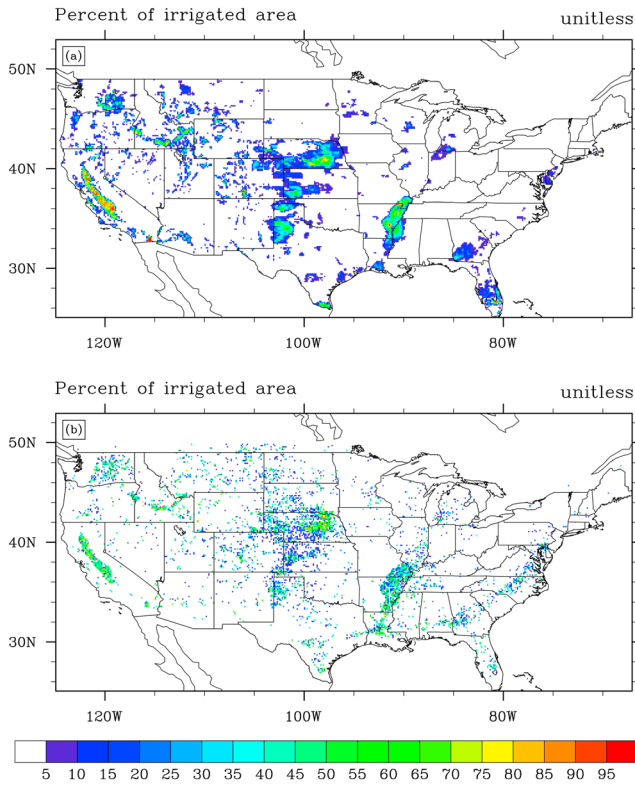


Figure 1. The percentage of each 0.125×0.125 grid cell defined as equipped for irrigation from (a) F_{GMIA} and (b) F_{MODIS} .

3. Results

3.1. Uncertainties From Irrigated Area Data Set

[19] Figures 1a and 1b show the spatial distributions of irrigation from F_{GMIA} and F_{MODIS} in CONUS, respectively. Both irrigation maps show remarkable agreement with a strong east-west divide. At the continental scale, major irrigated areas from both maps are distributed along the dry lowland valleys in California, Columbia River basin, and Snake River Basin of Idaho, as well as in the high mountains of Colorado. In central U.S., irrigation areas are found in the semiarid areas of western Kansas, Oklahoma, Texas, and Nebraska. In the Eastern parts of the country, irrigated land is mostly found along the Mississippi valley, agricultural regions of the eastern coastal plain and southwestern Georgia where high water demand crops such as cotton are planted. The F_{GMIA} map indicates that over 70% (by area) of all irrigated lands in the US are located in the semiarid western US, with smaller fraction of irrigated land in the eastern part of the country, where irrigation is supplemental to rain-fed crops.

[20] The F_{MODIS} map, as discussed in section 2.1, was derived from remotely sensed land surface properties and therefore is more observationally based but subject to uncertainties embedded in remote-sensing products. It estimates the total area equipped for irrigation in the continental U.S. to be $215,539 \text{ km}^2$, which shows a small bias of about 2% compared to the total irrigated area of $212,470 \text{ km}^2$ in $NASS_{2002}$ (Figure 2). In contrast, the F_{GMIA} map estimates the total irrigated area to be $267,282 \text{ km}^2$, which is about

25% larger than the $NASS_{2002}$. This may be due to the fact that F_{GMIA} for the U.S. was produced by assigning the maximum of the irrigated areas within a county as reported by the United States Geological Survey (USGS) and USDA census surveys, to agricultural land area provided by USGS and the United States Environmental Protection Agency at 30 m resolution [Siebert et al., 2005]. Consequently, irrigation fractions derived using such a procedure inherently suffer from positive biases. The estimated and reported irrigated areas for each water resources region are also given, which shows significant disagreement between the two data sets, especially in the eastern U.S., where irrigated areas from F_{GMIA} are generally high than $NASS_{2002}$, and vice versa from F_{MODIS} . High annual rainfall, the potential irrigation index derived from average annual inputs and a mixture of agricultural and natural vegetation, all made it difficult to distinguish irrigated cropland from rain-fed cropland using the Moderate Resolution Imaging Spectroradiometer (MODIS) based approach [Ozdogan and Gutman, 2008]. However, the pattern and fraction of irrigated area in major irrigated water resources regions such as Lower Mississippi, Arkansas White Red, and Texas show remarkable agreement with those reported in the $NASS_{2002}$ data set.

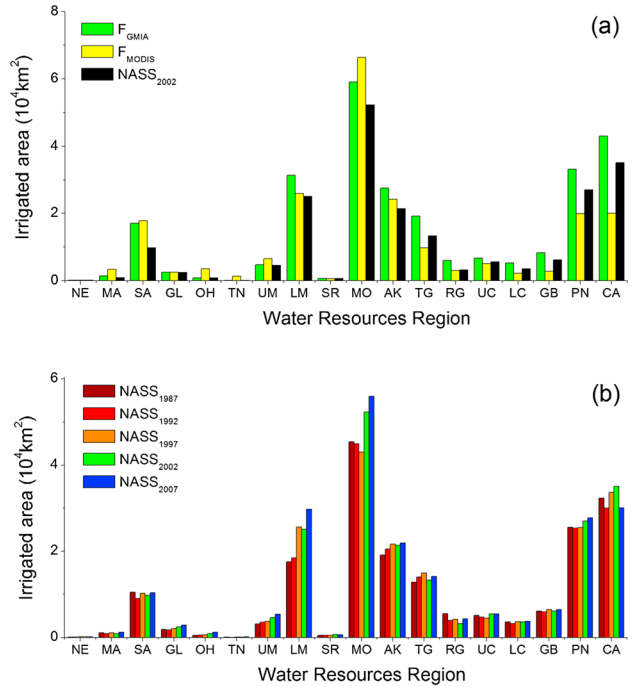


Figure 2. (a) Comparison of irrigated area in each water resources region from F_{GMIA} , F_{MODIS} , and $NASS_{2002}$, (b) temporal variations of irrigated area from $NASS$ with 5 year intervals from 1987–2007 for each water resource region. The horizontal axes denote the regions as defined in Figure S1 as follows. NE: New England, MA: Mid-Atlantic, SA: South Atlantic Gulf, GL: Great Lakes, OH: Ohio, TN: Tennessee, UM: Upper Mississippi, LM: Lower Mississippi, SR: Souris Red Rainy, MO: Missouri, AK: Arkansas White Red, TG: Texas Gulf, RG: Rio Grande, UC: Upper Colorado, LC: Lower Colorado, GB: Great Basin, PN: Pacific Northwest, CA: California.

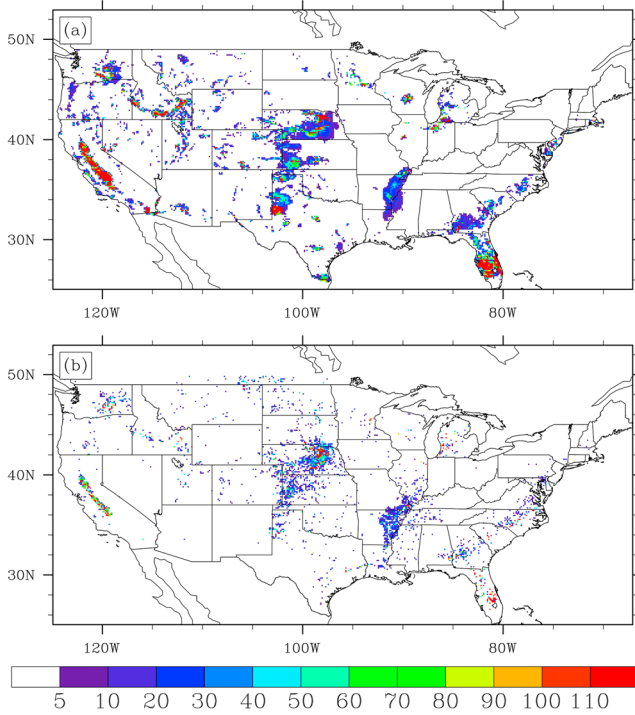


Figure 3. Spatial distribution of growing season (May–October) irrigation demands in mm/month by (a) $CLM_{GMIA,nocal}$ and (b) $CLM_{MODIS,nocal}$.

3.2. Experiments Before Calibration

[21] Figures 3a and 3b show the distribution of irrigation demand in the growing season (May–October) simulated by the $CLM_{GMIA,nocal}$ and $CLM_{MODIS,nocal}$, respectively. The simulated irrigation demand is concentrated over the western US, Mississippi, Missouri, and Texas Gulf, consistent with the spatial pattern of irrigated areas. The irrigation amounts from $CLM_{GMIA,nocal}$ and $CLM_{MODIS,nocal}$ are dominated by the western U.S. where the water demands

by crops cannot be met with the average annual precipitation below 20 in. The simulated irrigation demand is generally high in California, Pacific Northwest, Missouri, and Lower Mississippi with concentrated irrigated areas. Consistent with the difference in irrigated area, more irrigation demand is found in the western U.S. from CLM_{GMIA} than CLM_{MODIS} .

[22] Figure 4 shows the interannual variation of irrigation amounts simulated by $CLM_{GMIA,nocal}$ and $CLM_{MODIS,nocal}$ and that reported by NASS census data. Overall, the two noncalibrated CLM4 simulations show substantially higher irrigation demand in most major water resources regions compared to NASS. This suggests that the default F_{irrig} value calibrated based on global irrigation amount may not work well on a regional basis and emphasizes the need for calibration and validation in modeling studies. It is interesting to note that the irrigation demand in $CLM_{GMIA,nocal}$ is much higher than in $CLM_{MODIS,nocal}$ in Upper Colorado although the irrigated areas in this region from F_{GMIA} and F_{MODIS} generally agree with each other (Figure 2). This may be related to the large spatial variability of precipitation amount and seasonality in the continental mountainous areas so regional mean irrigation demands depend more on the spatial distribution of irrigated areas in relation to the precipitation than the total irrigated areas of the region. This highlights the importance of correctly estimating the spatial distribution of irrigated area in climatologically diverse regions.

3.3. Experiments With Parameter Calibration

[23] Figures 5a and 5b show the spatial distribution of the calibrated F_{irrig} values for each water resources region based on F_{GMIA} and F_{MODIS} , respectively. High values of F_{irrig} for F_{MODIS} are found in the western U.S. as the irrigated area is relatively low compared to NASS. The opposite is found for F_{irrig} for F_{GMIA} . Such differences between the calibrated F_{irrig} values based on different grid-based irrigated fraction products (i.e., F_{GMIA} and F_{MODIS}) are expected, given the same irrigation amount from NASS is used as the calibration target for a specific water

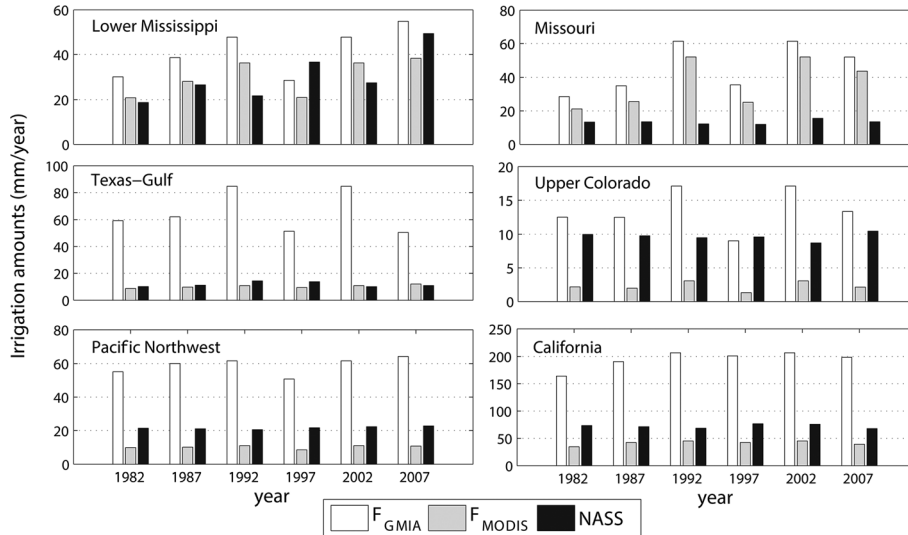


Figure 4. Comparison of simulated annual irrigation amounts by $CLM_{GMIA,nocal}$ (white) and $CLM_{MODIS,nocal}$ (gray) and the NASS census data (black).

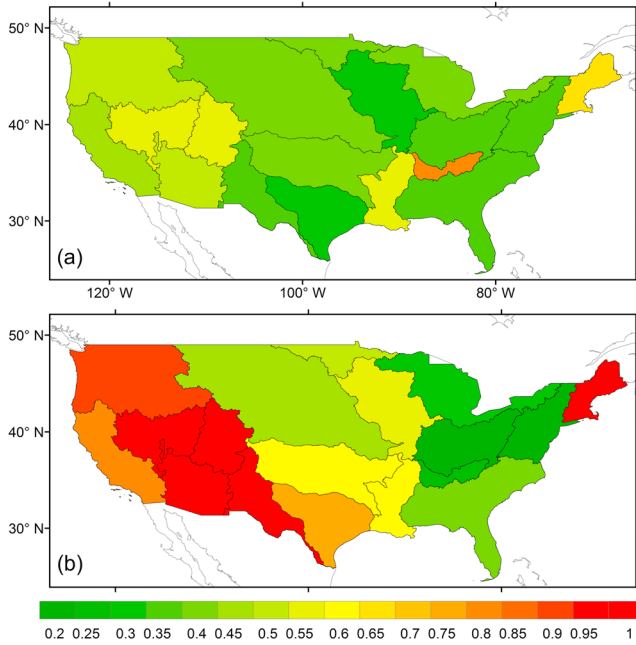


Figure 5. Spatial distributions of calibrated F_{irrig} values based on (a) F_{GMIA} and (b) F_{MODIS} .

resources region and the large discrepancy between F_{GMIA} and F_{MODIS} in terms of spatial distribution and magnitude as shown in Figure 1.

[24] Figures 6a and 6b show the spatial distribution of irrigation demand in the growing season simulated by the calibrated simulations, $\text{CLM}_{\text{GMIA,cal}}$ and $\text{CLM}_{\text{MODIS,cal}}$, respectively. Compared to the simulations before calibration, both $\text{CLM}_{\text{GMIA,cal}}$ and $\text{CLM}_{\text{MODIS,cal}}$ simulated lower irrigation demands after calibration that better capture the amplitude and interannual variations of irrigation amounts in the major water resources regions (Figure 7). With calibration, $\text{CLM}_{\text{GMIA,cal}}$ produced results generally closer to NASS than $\text{CLM}_{\text{MODIS,cal}}$.

[25] Irrigation effects simulated by models are dependent on their ability to simulate evapotranspiration (ET) at the land surface. Figure 8 shows a comparison between the simulated summertime (i.e., June, July, and August) ET from $\text{CLM}_{\text{noirrig}}$, $\text{CLM}_{\text{GMIA,cal}}$, $\text{CLM}_{\text{MODIS,cal}}$, and the MODIS data. From Figure 8, the simulated ET from $\text{CLM}_{\text{noirrig}}$, $\text{CLM}_{\text{GMIA,cal}}$, and $\text{CLM}_{\text{MODIS,cal}}$ all match the MODIS ET from *Tang et al.* [2009a, 2009b] estimates aggregated into model resolution (i.e., 0.125°) reasonably well in terms of spatial distribution and magnitude, but $\text{CLM}_{\text{GMIA,cal}}$ and $\text{CLM}_{\text{MODIS,cal}}$ show some improvements in simulating ET in agricultural areas such as the Central Valley, Columbia Basin, and the Arkansas Red river basin in general. To further evaluate the ET simulations, we compared the simulated and MODIS-based ET at the county level for all counties with an irrigation fraction greater than 0 in Figure 9. It is evident from Figure 9 that by adding irrigation, the mean annual ET fluxes simulated by CLM have smaller errors and correlate better with the MODIS ET than $\text{CLM}_{\text{noirrig}}$, even before calibration. The calibration further improved the performance of CLM simulations, with $\text{CLM}_{\text{GMIA,cal}}$ being the best performing model, followed by $\text{CLM}_{\text{MODIS,cal}}$.

3.4. Interannual Variability of Irrigation Impacts

[26] The impacts of irrigation on surface latent heat flux (LH), total runoff, and 10 cm soil temperature simulated by CLM4 with the calibrated parameters are examined. Figure 10 shows the irrigation impacts on LH in a relatively wet year (i.e., 1997), dry year (i.e., 2007), and climatology mean from 1979 to 2007 using F_{GMIA} and F_{MODIS} , respectively. More specifically for 2007 when irrigation amounts were larger than normal in general due to extreme drought and severe drought conditions prevailed in western U.S. and southeastern U.S., though wetter than normal conditions were still found in the South Central region (i.e., Texas Gulf) based on the Palmer Modified Drought Index from the National Climatic Data Center [Dai, 2011].

[27] In 2007, both $\text{CLM}_{\text{GMIA,cal}}$ and $\text{CLM}_{\text{MODIS,cal}}$ simulated large diurnal variation in the effects of irrigated agriculture on energy partitioning between sensible and latent heat fluxes. With irrigation, LH increases by $10\text{--}35\text{ W m}^{-2}$ from May through September during day time (16:00–02:00 UTC) in Missouri, Texas Gulf, Lower Mississippi, and Upper Colorado. The effects are most pronounced in Pacific Northwest, Lower Mississippi, and even more so in California, owing to a longer dry season that extend from May to October. To a lesser extent, midday LH increases with irrigation are also simulated in winter and spring of 2007 with anomalously low precipitation in California. Generally, $\text{CLM}_{\text{GMIA,cal}}$ simulated larger effects than $\text{CLM}_{\text{MODIS,cal}}$ in Lower Mississippi, Missouri, Upper Colorado, and Pacific Northwest, partly because $\text{CLM}_{\text{GMIA,cal}}$ simulated higher irrigation demand than $\text{CLM}_{\text{MODIS,cal}}$ (Figure 6). Local effects can be more extreme. For example, irrigation shifts over 50 W m^{-2} from

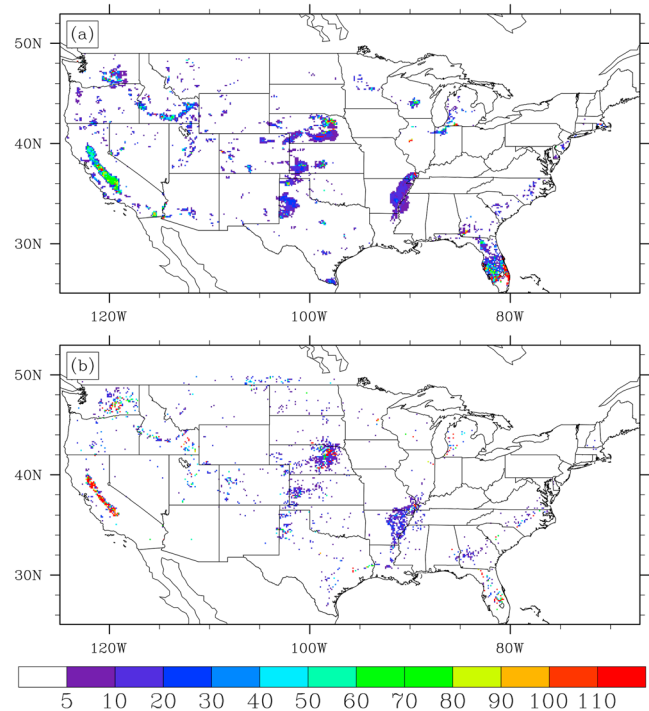


Figure 6. Spatial distribution of growing season (May–October) irrigation demands in mm/month by (a) $\text{CLM}_{\text{GMIA,cal}}$ and (b) $\text{CLM}_{\text{MODIS,cal}}$.

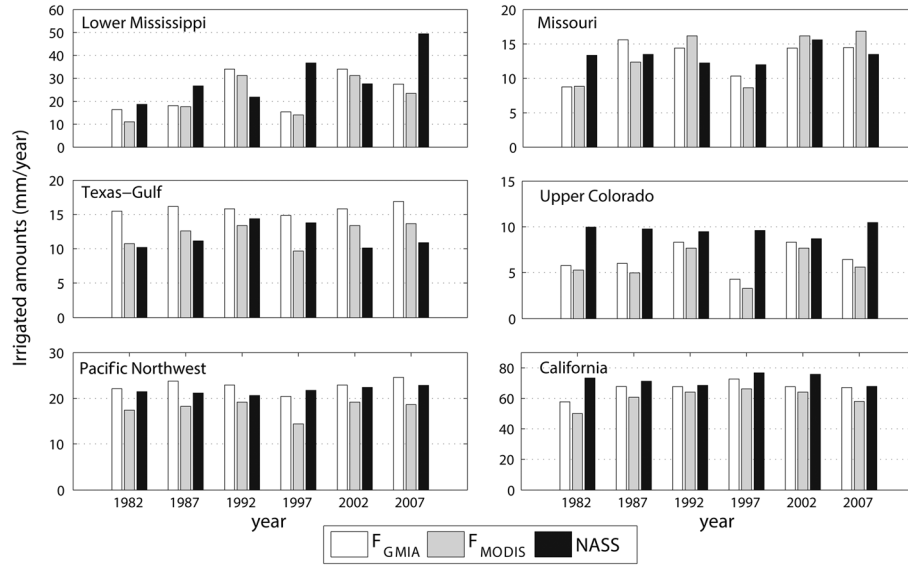


Figure 7. Comparison of simulated annual irrigation demand by $CLM_{GMIA,cal}$ (white) and $CLM_{MODIS,cal}$ (gray) with NASS census data (black).

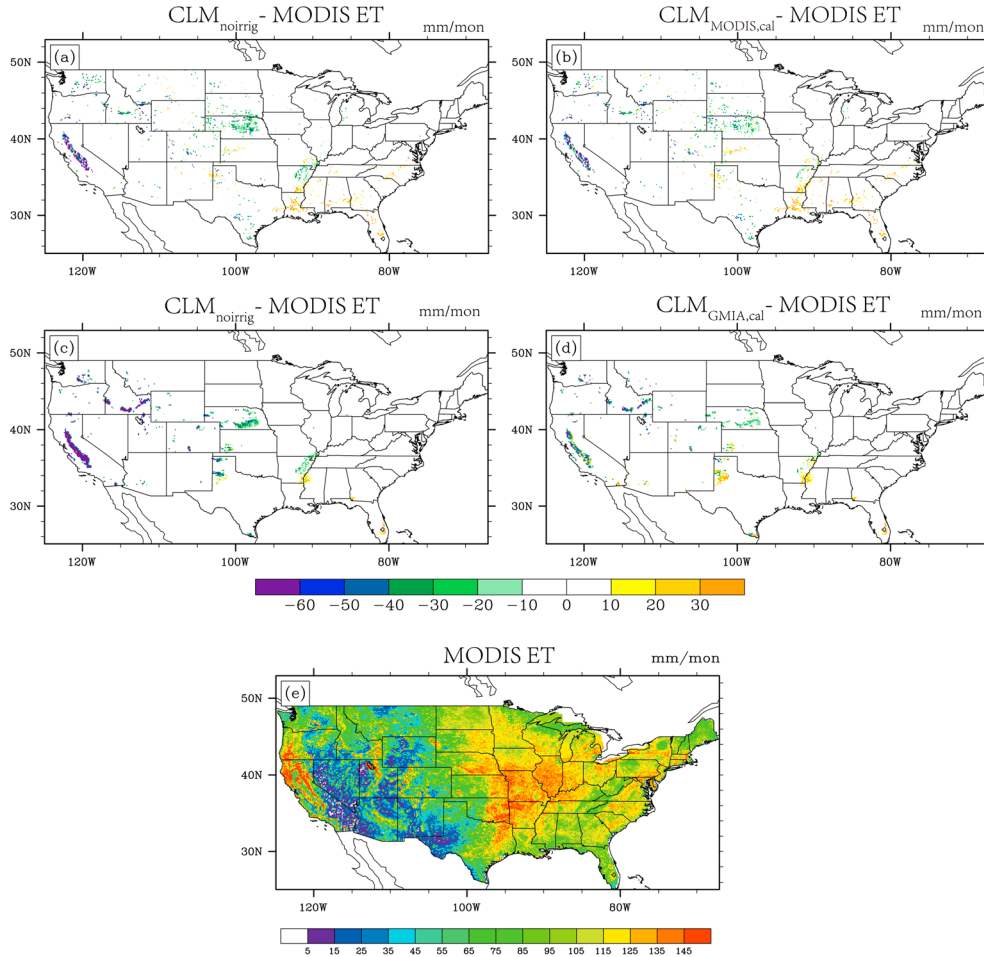


Figure 8. Difference of summer mean evapotranspiration between (e) MODIS ET and (a-d) simulated ET. Note that the no-irrigated grid cells in Figures 8a, 8b and Figures 8c, 8d are masked out using F_{MODIS} and F_{GMIA} data, respectively.

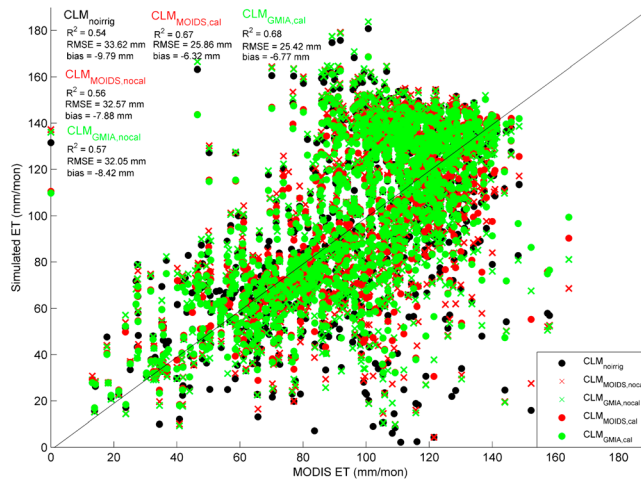


Figure 9. Simulated summer mean evapotranspiration from the CLM simulations compared against the MODIS data in 2001 at the county level.

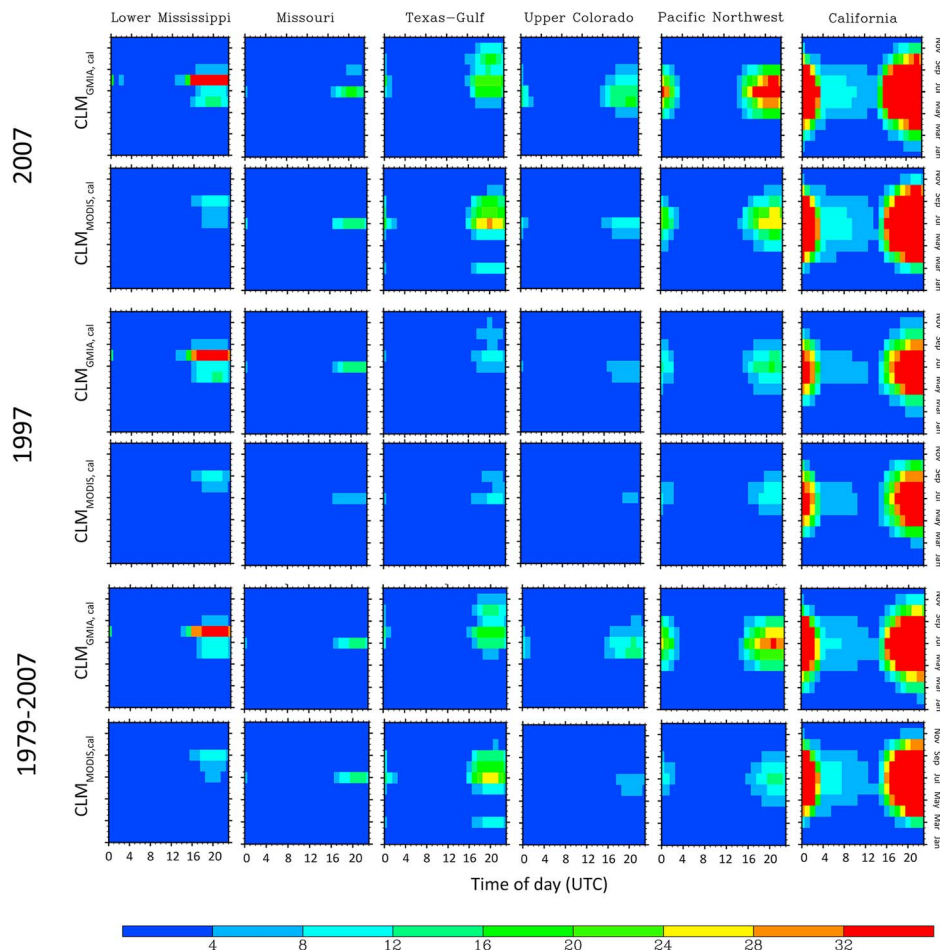


Figure 10. Difference of diurnal latent heat flux simulated by CLM between the irrigation and no irrigation (default) run in a dry year, 2007 (the top two panels) and wet year, 1997 (the middle two panels) and climatology mean for 1979–2007 (bottom two panels) for six water resource regions. The first, third, and fifth panels represent the results simulated by CLM_{GMIA,cal}, while the second, fourth, and sixth panels represent the results simulated by CLM_{MODIS,cal}.

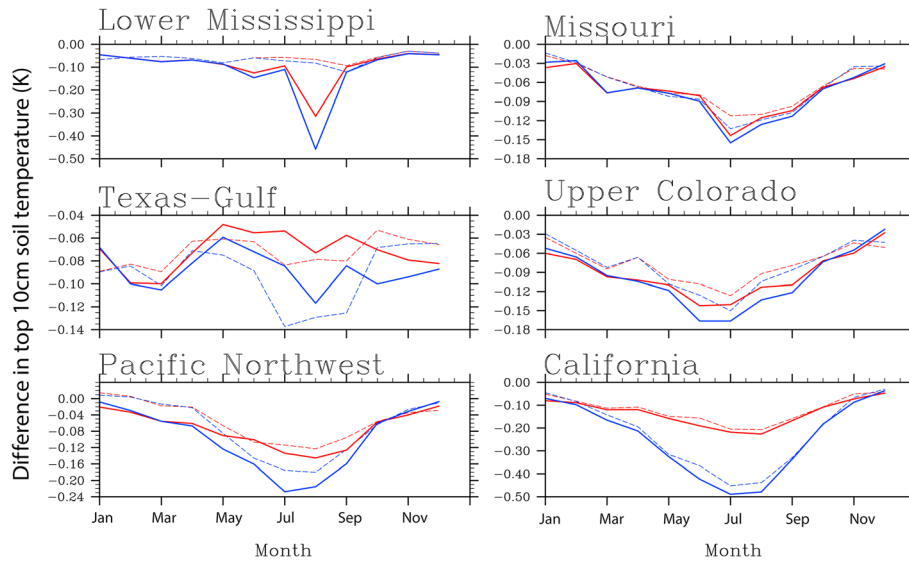


Figure 11. Difference of seasonal mean top 10 cm soil temperature simulated by $CLM_{GMIA, cal}$ (blue) and $CLM_{MODIS, cal}$ (red) and $CLM_{noirrig}$ run in dry year, 2007 (the solid line) and wet year, 1997 (the dashed line) for six water resources regions.

sensible heat to latent heat in the energy balance of many grid cells in California in July and August of the dry year. Effects of similar magnitude are also seen in eastern Lower Mississippi.

[28] Compared to 2007, both $CLM_{GMIA, cal}$ and $CLM_{MODIS, cal}$ show smaller effects in 1997, but large effects still exist in California and Lower Mississippi in 1997. At seasonal time scales, the effects of irrigation on energy partitioning appear to be large and persistent and more pronounced in dry years when reduced precipitation and higher evaporative losses drive higher irrigation demands.

[29] Figure 11 shows the irrigation impacts on the top 10 cm soil temperature in 1997 and 2007 simulated by

$CLM_{GMIA, cal}$ and $CLM_{MODIS, cal}$. Irrigation raises the soil water content, enabling evapotranspiration, which lower the temperature. In general, peak decrease in the 10 cm soil temperature occurred in July and August when changes in LH are largest (Figure 10). In California and Lower Mississippi, the 10 cm soil temperature decreases by 0.5 K during the summer peak. Consistent with the higher irrigation amounts and larger increase in LH, the simulated decrease of 10 cm soil temperature by $CLM_{GMIA, cal}$ is larger than $CLM_{MODIS, cal}$.

[30] Figure 12 shows the irrigation impacts on the total runoff in 1997 and 2007 simulated by $CLM_{GMIA, cal}$ and $CLM_{MODIS, cal}$. Even though we have calibrated the model

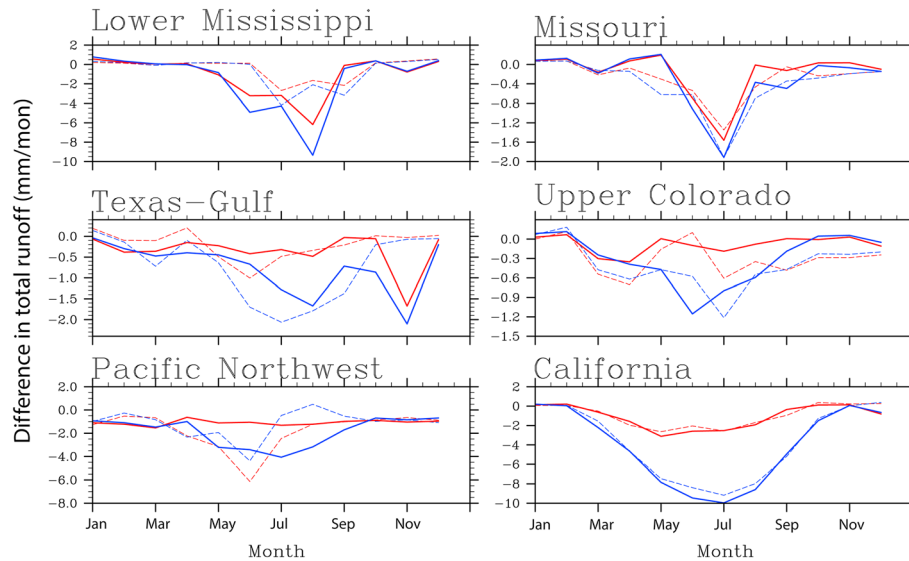


Figure 12. Difference of seasonal mean total runoff simulated by $CLM_{GMIA, cal}$ (blue) and $CLM_{MODIS, cal}$ (red) and $CLM_{noirrig}$ run in dry year, 2007 (the solid line) and wet year, 1997 (the dashed line) for six water resources regions.

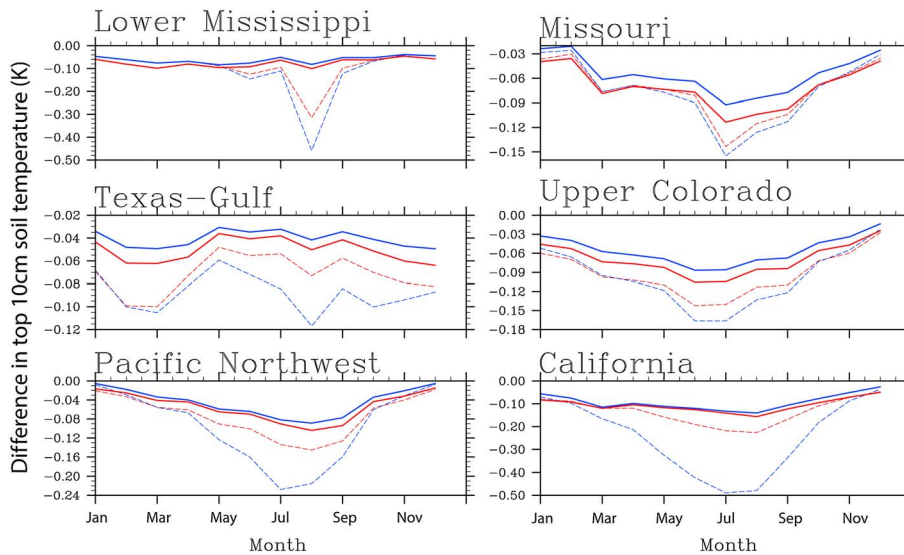


Figure 13. Difference of seasonal mean top 10 cm soil temperature simulated by $CLM_{GMIA,con}$ (blue) and $CLM_{MODIS,con}$ (red) and $CLM_{noirrig}$ run in 2007. The solid line represents the simulation results after constraining irrigation amounts by the water availability, while the dashed line represents the results assuming the water for irrigation was available whenever needed.

parameters to yield overall good agreement with NASS for both simulations, their differences still dominate the interannual differences in runoff response. For example, with F_{MODIS} , the interannual variability of irrigation impacts on runoff is smaller over all river basins in the western US compared to using F_{GMIA} because the fractional irrigated area of the former is much smaller. This has important implications to modeling irrigation impacts and potential feedbacks in extreme conditions. We note that our estimates of irrigation effect on runoff fall within the range of previous studies when averaged over the continental scale or large river basins. By assuming water for irrigation was always available, *Ozdogan et al.* [2010] showed that irrigation could lead to runoff changes by 0.01 mm d^{-1} ($\sim 0.3 \text{ mm month}^{-1}$) when averaged over the continental U.S.; *Haddeland et al.* [2006] estimated that irrigation could lead to runoff changes from 42.3 mm yr^{-1} to 26.5 mm yr^{-1} ($\sim 1.3 \text{ mm month}^{-1}$) and from 734 mm yr^{-1} to 716 mm yr^{-1} ($\sim 1.5 \text{ mm month}^{-1}$) for the Colorado and Mekong river basins, respectively.

3.5. Experiments With the Constraints of Local Water Availability

[31] In all the experiments reported so far, water is assumed to be available whenever needed to meet the irrigation demand. In other words, the irrigation demand calculated as a deficit between the soil moisture target in equation (1) and the soil moisture status at 6 A.M. of each day in the growing season is assumed to be always met by extracting water from the total runoff in the same grid cell. This could result in negative total runoff values under extreme conditions when the irrigation demand exceeds the total runoff at the given grid cell, which is not realistic but numerically allowed. Therefore, the CLM4 irrigation scheme only represents a first step toward a realistic representation of hydrology and water resources management practices in the real world. To achieve such a representation, substantial model developments are needed, including groundwater pumping, runoff and streamflow

routing, and reservoir operation, which are out of the scope of this study but have been reported in a series of follow-up studies [i.e., *Leng et al.*, 2013; *Li et al.*, 2013; *Voisin et al.*, 2013]. Briefly, sources of water for irrigation (i.e., groundwater versus surface water), routing of water along the flow path from hillslopes and subsurface systems into tributaries and then into major streams, and the storage and distribution of water in and from reservoirs are all important factors to be considered to understand water availability to satisfy irrigation demands at local and regional scales. Interested readers are referred to these papers for details.

[32] In this study, the impacts of extreme conditions when the local total runoff cannot provide surface water to meet the irrigation water demand is explored in a simplistic way using the dry year 2007 as a case study to investigate irrigation effects with the constraints of local water availability at the intraseasonal time scale.

[33] As discussed earlier, this experiment represents the opposite extreme from previous experiments where water is always available in that we assume water can only come from the liquid runoff of the local grid cell. Comparing the experiments with unlimited water availability and constrained water availability by local water supply can provide a range of irrigation impacts that bracket the reality when irrigation can be limited by availability from water storage such as streams, reservoirs, and groundwater. From $CLM_{GMIA,con}$ and $CLM_{MODIS,con}$ (i.e., the two 1 year simulations in Table 1), the magnitude of irrigation impacts are reduced significantly when irrigation is constrained by local water availability, especially in California, Lower Mississippi, and Pacific Northwest where extreme and severe droughts occurred in 2007 (Figures 13 and 14). Most previous studies did not consider water availability for irrigation and assumed that water was always available to meet irrigation demands [*Ozdogan et al.*, 2010; *Sacks et al.*, 2009]. Limited by local water availability, the energy and water balance components are influenced by irrigation in the same direction as

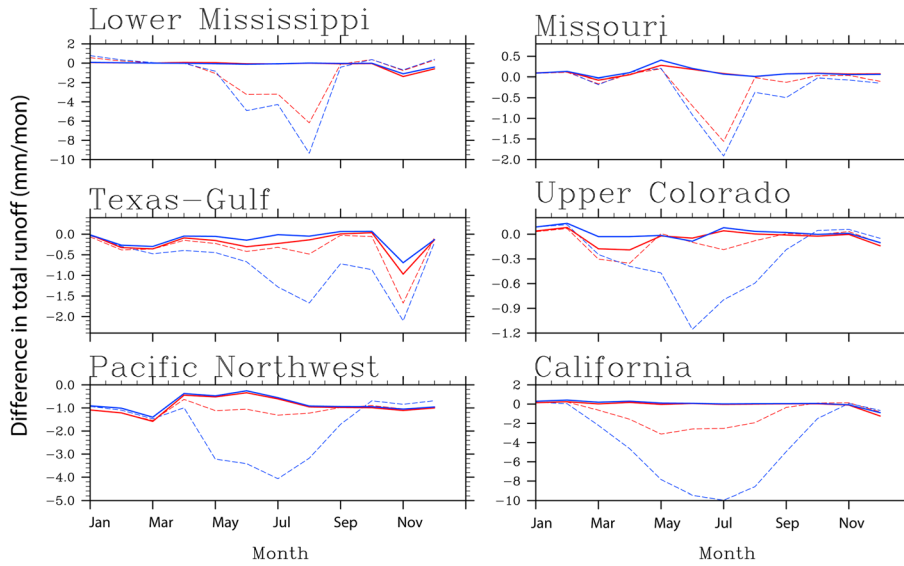


Figure 14. Difference of seasonal mean total runoff simulated by $CLM_{GMIA,con}$ (blue) and $CLM_{MODIS,con}$ (red) and $CLM_{noirrig}$ run in 2007. The solid line represents the simulation results after constraining irrigation amounts by the water availability, while the dashed line represents the results assuming the water for irrigation was available whenever needed.

simulations with no constraint of water availability, but with more moderate effects. For example, the change in 10 m soil temperature becomes negligible in California in 2007 when local water availability is considered, which reduces the irrigation amounts, resulting in less root uptake and transpiration, and much smaller effects of irrigation.

4. Conclusion and Discussion

[34] Previous studies generally investigated irrigation effects based on sensitivity experiments. For example, *Kueppers et al.* [2007] forced the RegCM3 model root zone (top 1 m) soil moisture to field capacity every time step to simulate irrigation effects. *Kanamaru and Kanamitsu* [2008] investigated the effects of irrigation on regional climate using the Regional Spectral Model by prescribing root zone soil moisture to 100% and 50% saturated conditions respectively at each time step and compared their differences. *Lobell et al.* [2009] using the Community Atmospheric Model (i.e., CAM3.3), prescribed the top 30 cm soil moisture in each irrigated grid cell to values from 30% to 90% of the soil saturation. *Boucher et al.* [2004] and *Sacks et al.* [2009] applied realistic irrigation amounts constrained by observations to simulate irrigation effects. However, the irrigation schemes they used are less realistic in that *Boucher et al.* [2004] directly prescribed rather than simulated the evapotranspiration flux from irrigation and *Sacks et al.* [2009] applied irrigation evenly throughout the growing season regardless of the soil moisture state. Depending on each model's parameterizations and input uncertainties especially at the regional scale, previous studies may yield ambiguous interpretation of the irrigation's effect on regional climate. However, since the simulated irrigation amounts were usually not reported in previous studies, model uncertainty cannot be evaluated.

[35] In this study, the effects of irrigation in the continental U.S. on surface fluxes and land surface states are examined

using two different irrigation fraction data sets as inputs to CLM4 with model calibration using the NASS census data. The following is a summary of our findings.

[36] 1. Relative to the NASS census data, large discrepancy and uncertainties exist between the grid-based F_{GMIA} and F_{MODIS} data, which are important sources of uncertainty in modeling irrigation effects. Even with model calibration to yield overall good agreement with NASS, differences between F_{GMIA} and F_{MODIS} still dominate the differences in the interannual variability of land surface response to irrigation. With smaller irrigation fractional area in the F_{MODIS} data, interannual variability of the impacts of irrigation is smaller compared to using the F_{GMIA} data. This has important implications to modeling irrigation impacts in extreme conditions. Furthermore, even if both data sets agree on the total irrigated areas in a region, the total irrigation demands can still be very different in regions with large spatial variability of precipitation amount and seasonality. Since both data sets are subject to uncertainties associated with either the source data or methods used to derive them, it is critical to acknowledge and characterize/quantify uncertainties that propagated through the models in any impact studies using these data sets. Results from this study also highlight the importance of improving the estimates of the intensity and spatial distribution of irrigated area in modeling irrigation demands and impacts.

[37] 2. Our results suggest that the irrigation demands simulated by $CLM_{GMIA,nocal}$ and $CLM_{MODIS,nocal}$ using the default value of the F_{irrig} parameter previously obtained based on calibration of global gross irrigation withdrawal are both unreasonably high compared to NASS. After calibration using the NASS census data, $CLM_{GMIA,cal}$ and $CLM_{MODIS,cal}$ both more reliably simulated the irrigation demands in heavily irrigated water resources regions in term of amplitude and temporal variation. This suggests that global calibration of the F_{irrig} parameter may not capture large regional differences in irrigation amounts. By constraining

model performance using observations, we demonstrate that the performance of the irrigation scheme can be improved through calibration of model parameters.

[38] 3. With the calibrated parameters assigned to each grid, our results indicate that the effects of irrigation in the growing season on land surface fluxes and states are more pronounced in dry years, with more significant effects occurring locally at daytime.

[39] 4. By accounting for water availability, our tests indicate that the magnitude of irrigation effects is greatly reduced. Hence, in addition to irrigation data sets and model parameters, water availability for irrigation is another important factor that should be considered in assessing the impacts of irrigation. To more realistically represent water availability for irrigation, the effects of reservoirs on regulating streamflow should be considered to account for water supply from local and remote storages.

[40] Overall, by constraining model performance using observations, this study demonstrates that the performance of the CLM4 irrigation scheme can be improved through parameter calibration. However, uncertainty in the irrigation area data must be reduced to further reduce uncertainty in simulating irrigation effects at the seasonal to interannual time scales. Through the water availability experiments, we evaluated the deficiency in the current parameterization and point out a critical path forward to a realistic assessment of irrigation impacts using an earth system modeling approach. A more complete parameterization to simulate crop irrigation demands by incorporating phenological development with crop-specific parameters has been incorporated into later versions of CLM [Levis *et al.*, 2012; Oleson *et al.*, 2013]. Levis *et al.* [2012] demonstrated that by replacing the CLM's unmanaged "grass-like" crop with managed corn, soybean, and temperate cereals as in Integrated Biosphere Simulator agricultural version [Kucharik and Brye, 2003], the coupled Community Atmospheric Model version 4 (CAM4)-CLM4 simulated significant changes in North American temperature and precipitation due to changes in the turbulent heat fluxes associated with improved leaf area index simulations of crops. However, irrigation was not considered in that study, which might have contributed to the overestimation of Midwestern North American temperatures in summer in their simulations. Nevertheless, their results suggest that crop-specific parameters may have important influence on ET and hence the assumption of a grass-like generic crop type in this study may have effects on our simulated irrigation effects that deserve further investigation in the future.

[41] Furthermore, the assumption that water resources are freely available for irrigation and the lack of representations of factors controlling water supply for irrigation need to be relaxed and considered. For example, the water constraint experiments, CLM_{GMA,con} and CLM_{MODIS,con}, were conducted based on the assumption that irrigation water could be only extracted from local runoff (i.e., Q_{runoff}), which is oversimplified compared to real-world scenarios in which irrigation water could be from rivers, reservoirs, and groundwater withdrawal. In addition, the model also assumes 100% irrigation efficiency, that is, the amount of water reaching the root zone of the plants is the same as the amount of water taken from the source (river, well). As with most other irrigation schemes used in land surface models, these

limitations contribute to uncertainties in modeling irrigation impacts and should be further investigated in future studies. Therefore, to understand the complex interactions between climate, irrigation, and cropping systems, further research on this topic should be pursued using an Earth system approach.

[42] Significant efforts have been made toward this path and have been reported in separate publications. A groundwater pumping scheme has been developed and implemented into CLM [Leng *et al.*, 2013]; a physically based river routing module, the Model for Scale Adaptive River Transport (MOSART), has been developed and coupled with CLM [Li *et al.*, 2013]; a water management module that simulate reservoir operations using operational rules with competing targets has been developed and coupled with CLM and MOSART [Voisin *et al.*, 2013].

[43] Although this study is performed using offline CLM simulations, it has important implications to coupled simulations since our results show that the irrigation amounts, hence surface fluxes, can be very sensitive to the irrigation areas and parameters used in the irrigation scheme. With offline simulations, however, the response of ET to irrigation may differ from that derived from coupled simulations. This difference is likely dependent on the role of land-atmosphere feedbacks on surface fluxes and boundary layer and cloud development. In regions such as the Central U.S. where land-atmosphere coupling strength is stronger [Koster *et al.*, 2004], it may be more important to use coupled models to study irrigation effects. Hence, to quantify climate/hydrologic/ecological consequences of irrigation at regional and global scales, studies using coupled land-atmosphere models that include more realistic representations of irrigation amounts as well as sources in a modeling framework that integrates with river routing and water management will be pursued in the future.

[44] **Acknowledgments.** This study was supported by the Integrated Earth System Modeling (iESM) project funded by Department of Energy Earth System Modeling program. The Pacific Northwest National Laboratory (PNNL) Platform for Regional Integrated Modeling and Analysis (PRIMA) Initiative provided the model configuration and data sets used in the numerical experiments. PNNL is operated by Battelle Memorial Institute for the U.S. Department of Energy under contract DE-AC05-76RLO1830. This work was also partly funded by the National Natural Science Foundation of China (41171031) and the National Basic Research Program of China (2012CB955403).

References

- Adegoke, J. O., R. A. Pielke Sr., J. Eastman, R. Mahmood, and K. G. Hubbard (2003), Impact of irrigation on midsummer surface fluxes and temperature under dry synoptic conditions: A regional atmospheric model study of the US High Plains, *Mon. Weather Rev.*, *131*(3), 556–564, doi:10.1175/1520-0493(2003)131<0556:IOIOMS>2.0.CO;2.
- Anderson, R. G., M. H. Lo, and J. S. Famiglietti (2012), Assessing surface water consumption using remotely sensed groundwater, evapotranspiration, and precipitation, *Geophys. Res. Lett.*, *39*, L16401, doi:10.1029/2012GL052400.
- Biggs, T. W., C. A. Scott, A. Gaur, J.-P. Venot, T. Chase, and E. Lee (2008), Impacts of irrigation and anthropogenic aerosols on the water balance, heat fluxes, and surface temperature in a river basin, *Water Resour. Res.*, *44*, W12415, doi:10.1029/2008WR006847.
- Bonfils, C., and D. Lobell (2007), Empirical evidence for a recent slowdown in irrigation-induced cooling, *Proc. Natl. Acad. Sci. U. S. A.*, *104*(34), 13,582–13,587, doi:10.1073/pnas.0700144104.
- Boucher, O., G. Myhre, and A. Myhre (2004), Direct human influence of irrigation on atmospheric water vapour and climate, *Clim. Dyn.*, *22*(6), 597–603, doi:10.1007/s00382-004-0402-4.

- Cheng, L., Z. Xu, D. Wang, and X. Cai (2011), Assessing interannual variability of evapotranspiration at the catchment scale using satellite-based evapotranspiration data sets, *Water Resour. Res.*, *47*, W09509, doi:10.1029/2011WR010636.
- Clapp, R. B., and G. M. Hornberger (1978), Empirical equations for some soil hydraulic properties, *Water Resour. Res.*, *14*(4), 601–604, doi:10.1029/WR014i004p00601.
- Collins, W. D., et al. (2006), The Community Climate System Model Version 3 (CCSM3), *J. Clim.*, *19*, 2122–2143, doi:10.1175/JCLI3761.1.
- Cosgrove, B. A., et al. (2003), Land surface model spin-up behavior in the North American Land Data Assimilation System (NLDAS), *J. Geophys. Res.*, *108*(D22), 8845, doi:10.1029/2002JD00331603.
- Dai, A. (2011), Characteristics and trends in various forms of the Palmer Drought Severity Index during 1900–2008, *J. Geophys. Res.*, *116*, D12115, doi:10.1029/2010JD015541.
- DeAngelis, A., F. Dominguez, Y. Fan, A. Robock, M. D. Kustu, and D. Robinson (2010), Evidence of enhanced precipitation due to irrigation over the Great Plains of the United States, *J. Geophys. Res.*, *115*, D15115, doi:10.1029/2010JD013892.
- Diffenbaugh, N. S. (2009), Influence of modern land cover on the climate of the United States, *Clim. Dyn.*, *33*(7–8), 945–958, doi:10.1007/s00382-009-0566-z.
- Douglas, E. M., D. Niyogi, S. Frolking, J. Yeluripati, R. A. Pielke Sr., N. Niyogi, C. Vörösmarty, and U. Mohanty (2006), Changes in moisture and energy fluxes due to agricultural land use and irrigation in the Indian Monsoon Belt, *Geophys. Res. Lett.*, *33*, L14403, doi:10.1029/2006GL026550.
- Douglas, E. A., Beltrán-Przekurat, D. Niyogi, R. Pielke Sr., and C. Vörösmarty (2009), The impact of agricultural intensification and irrigation on land-atmosphere interactions and Indian monsoon precipitation—A mesoscale modeling perspective, *Global Planet. Change*, *67*(1–2), 117–128, doi:10.1016/j.gloplacha.2008.12.007.
- Famiglietti, J. S., M. Lo, S. L. Ho, J. Bethune, K. J. Anderson, T. H. Syed, S. C. Swenson, C. R. de Linage, and M. Rodell (2011), Satellites measure recent rates of groundwater depletion in California's Central Valley, *Geophys. Res. Lett.*, *38*, L03403, doi:10.1029/2010GL046442.
- Franks, S. W., K. J. Beven, P. F. Quinn, and I. R. Wright (1997), On the sensitivity of soil-vegetation-atmosphere transfer (SVAT) schemes: Equifinality and the problem of robust-calibration, *Agric. For. Meteorol.*, *86*(1–2), 63–75.
- Gao, H., Q. Tang, C. R. Ferguson, E. F. Wood, and D. P. Lettenmaier (2010), Estimating the water budget of major US river basins via remote sensing, *Int. J. Remote Sens.*, *31*(14), 3955–3978, doi:10.1080/01431161.2010.483488.
- Gent, P., S. Yeager, R. Neale, S. Levis, and D. Bailey (2010), Improvements in a half degree atmosphere/land version of the CCSM, *Clim. Dyn.*, *34*(6), 819–833, doi:10.1007/s00382-009-0614-8.
- Gordon, L. J., W. Steffen, B. F. Jonsson, C. Folke, M. Falkenmark, and A. Johannessen (2005), Human modification of global water vapor flows from the land surface, *Proc. Natl. Acad. Sci. U. S. A.*, *102*(21), 7612–7617, doi:10.1073/pnas.0500208102.
- Haddeland, I., D. P. Lettenmaier, and T. Skaugen (2006), Effects of irrigation on the water and energy balances of the Colorado and Mekong river basins, *J. Hydrol.*, *324*(1–4), 210–223, doi:10.1016/j.jhydrol.2005.09.028.
- Hanasaki, N., S. Kanae, and T. Oki (2006), A reservoir operation scheme for global river routing models, *J. Hydrol.*, *327*(1–2), 22–41, doi:10.1016/j.jhydrol.2005.11.011.
- Kanamaru, H., and M. Kanamitsu (2008), Model diagnosis of nighttime minimum temperature warming during summer due to irrigation in the California Central Valley, *J. Hydrometeorol.*, *9*(5), 1061–1072, doi:10.1175/2008JHM967.1.
- Kawase, H., T. Yoshikane, M. Hara, F. Kimura, T. Sato, and S. Ohsawa (2008), Impact of extensive irrigation on the formation of cumulus clouds, *Geophys. Res. Lett.*, *35*, L01806, doi:10.1029/2007GL032435.
- Ke, Y., R. L. Leung, M. Huang, A. M. Coleman, H. Li, and M. S. Wigmosta (2012), Developing high resolution land surface parameters for Community Land Model, *Geosci. Model Dev.*, *5*, 1435–1481, doi:10.5194/gmd-5-1435-2012.
- Koster, R. D., P. A. Dirmeyer, Z. Guo, G. Bonan, E. Chan, P. Cox, C. Gordon, S. Kanae, E. Kowalczyk, and D. Lawrence (2004), Regions of strong coupling between soil moisture and precipitation, *Science*, *305*(5687), 1138–1140, doi:10.1126/science.1100217.
- Kucharik, C. J., and K. R. Brye (2003), Integrated Biosphere Simulator (IBIS) yield and nitrate loss predictions for Wisconsin maize receiving varied amounts of nitrogen fertilizer, *J. Environ. Qual.*, *32*, 247–268.
- Kueppers, L. M., and M. A. Snyder (2011), Influence of irrigated agriculture on diurnal surface energy and water fluxes, surface climate, and atmospheric circulation in California, *Clim. Dyn.*, *38*(5–6), 1017–1029, doi:10.1007/s00382-011-1123-0.
- Kueppers, L. M., M. A. Snyder, L. C. Sloan, D. Cayan, J. Jin, H. Kanamaru, M. Kanamitsu, N. L. Miller, M. Tyree, H. Du, and B. Weare (2008), Seasonal temperature responses to land-use change in the western United States, *Global Planet. Change*, *60*, 250–264, doi:10.1016/j.gloplacha.2007.03.005.
- Kueppers, L. M., M. A. Snyder, and L. C. Sloan (2007), Irrigation cooling effect: Regional climate forcing by land-use change, *Geophys. Res. Lett.*, *34*, L03703, doi:10.1029/2006GL028679.
- Kustu, M. D., Y. Fan, and A. Robock (2010), Large-scale water cycle perturbation due to irrigation pumping in the US High Plains: A synthesis of observed streamflow changes, *J. Hydrol.*, *390*(3–4), 222–244, doi:10.1016/j.jhydrol.2010.06.045.
- Lawrence, D., et al. (2011a), Parameterization improvements and functional and structural advances in version 4 of the Community Land Model, *J. Adv. Model. Earth Syst.*, *3*, M03001, doi:10.1029/2011MS000045.
- Lawrence, D. M., K. W. Oleson, M. G. Flanner, C. G. Fletcher, P. J. Lawrence, S. Levis, S. C. Swenson, and G. B. Bonan (2011b), The CCSM4 Land Simulation, 1850–2005: Assessment of surface climate and new capabilities, *J. Clim.*, *25*(7), 2240–2260, doi:10.1175/JCLI-D-11-00103.1.
- Lee, E., T. N. Chase, B. Rajagopalan, R. G. Barry, T. W. Biggs, and P. J. Lawrence (2009), Effects of irrigation and vegetation activity on early Indian summer monsoon variability, *Int. J. Climatol.*, *29*(4), 573–581, doi:10.1002/joc.1721.
- Leng G., M. Huang, Q. Tang, and L. Y. R. Leung (2013), Modeling the effects of groundwater-fed irrigation on terrestrial hydrology over the conterminous United States, *J. Hydrometeorol.*, in review.
- Levis, S., G. B. Bonan, E. Kluzek, P. E. Thornton, A. Jones, W. J. Sacks, and C. J. Kucharik (2012), Interactive Crop Management in the Community Earth System Model (CESM1): Seasonal influences on land-atmosphere fluxes, *J. Clim.*, *25*, 4,835–4,859, doi:10.1175/JCLI-D-11-00446.1.
- Li, H., M. S. Wigmosta, H. Wu, M. Huang, Y. Ke, A. M. Coleman, and L. R. Leung (2013), A physically based runoff routing model for land surface and Earth system models, *J. Hydrometeorol.*, *14*, 808–828, doi:10.1175/JHM-D-12-015.1.
- Lobell, D. B., C. Bonfils, and J.-M. Faurès (2008), The role of irrigation expansion in past and future temperature trends, *Earth Interact.*, *12*(3), 1–11, doi:10.1175/2007EI241.1.
- Lobell, D., G. Bala, A. Mirin, T. Phillips, R. Maxwell, and D. Rotman (2009), Regional differences in the influence of irrigation on climate, *J. Clim.*, *22*(8), 2248–2255, doi:10.1175/2008JCLI2703.1.
- Oleson K. W., et al. (2010), Technical description of version 4.0 of the Community Land Model (CLM), NCAR Technical Note NCAR/TN-478 +STR, 257 pp.
- Oleson, K. E., et al. (2013), Technical description of version 4.5 of the Community Land Model (CLM), June 2013, National Center for Atmospheric Research, Boulder, CO. http://www.cesm.ucar.edu/models/cesm1.2/clm/CLM45_Tech_Note.pdf.
- Ozdogan, M., and G. Gutman (2008), A new methodology to map irrigated areas using multi-temporal MODIS and ancillary data: An application example in the continental US, *Remote Sens. Environ.*, *112*(9), 3520–3537, doi:10.1016/j.rse.2008.04.010.
- Ozdogan, M., M. Rodell, H. K. Beaudoin, and D. L. Toll (2010), Simulating the effects of irrigation over the United States in a land surface model based on satellite-derived agricultural data, *J. Hydrometeorol.*, *11*(1), 171–184, doi:10.1175/2009JHM1116.1.
- Pielke, R., Sr., J. Adegoke, A. Beltran-Przekurat, C. A. Hiemstra, J. Lin, U. S. Nair, D. Niyogi, and T. E. Nobis (2007), An overview of regional land-use and land-cover impacts on rainfall, *Tellus B*, *59*(3), 587–601, doi:10.1111/j.1600-0889.2007.00251.x.
- Puma, M. J., and B. I. Cook (2010), Effects of irrigation on global climate during the 20th century, *J. Geophys. Res.*, *115*, D16120, doi:10.1029/2010JD014122.
- Qian, Y., M. Huang, B. Yang, and L. K. Berg (2013), A modeling study of irrigation effects on surface fluxes and land-air-cloud interactions in the Southern Great Plains, *J. Hydrometeorol.*, *14*, 700–721, doi:10.1175/JHM-D-12-0134.1.
- Sacks, W. J., B. I. Cook, N. Buening, S. Levis, and J. H. Helkowski (2009), Effects of global irrigation on the near-surface climate, *Clim. Dyn.*, *33*(2–3), 159–175, doi:10.1007/s00382-008-0445-z.
- Saeed, F., S. Hagemann, and D. Jacob (2009), Impact of irrigation on the South Asian summer monsoon, *Geophys. Res. Lett.*, *36*, L20711, doi:10.1029/2009GL040625.
- Segal, M., Z. Pan, R. Turner, and E. Takle (1998), On the potential impact of irrigated areas in North America on summer rainfall caused by large-scale systems, *J. Appl. Meteorol.*, *37*(3), 325–331, doi:10.1175/1520-0450-37.3.325.
- Shibuo, Y., J. Jarsjö, and G. Destouni (2007), Hydrological responses to climate change and irrigation in the Aral Sea drainage basin, *Geophys. Res. Lett.*, *34*, L21406, doi:10.1029/2007GL031465.
- Shiklomanov, I. A. (2000), Appraisal and assessment of world water resources, *Water Int.*, *25*, 11–32, doi:10.1080/02508060008686794.

- Siebert, S., P. Döll, J. Hoogeveen, J. M. Faures, K. Frenken, and S. Feick (2005), Development and validation of the global map of irrigation areas, *Hydrol. Earth Syst. Sci.*, 9(5), 535–547, doi:10.5194/hess-9-535-2005.
- Sorooshian, S., J. Li, K.-I. Hsu, and X. Gao (2011), How significant is the impact of irrigation on the local hydroclimate in California's Central Valley? Comparison of model results with ground and remote-sensing data, *J. Geophys. Res.*, 116, D06102, doi:10.1029/2010JD014775.
- Sorooshian, S., J. Li, K. Hsu, and X. Gao (2012), Influence of irrigation schemes used in regional climate models on evapotranspiration estimation: Results and comparative studies from California's Central Valley agricultural regions, *J. Geophys. Res.*, 117, D06107, doi:10.1029/2011JD016978.
- Tang, Q., T. Oki, S. Kanae, and H. Hu (2007), The influence of precipitation variability and partial irrigation within grid cells on a hydrological simulation, *J. Hydrometeorol.*, 8(3), 499–512, doi:10.1175/JHM589.1.
- Tang, Q., E. Rosenberg, and D. Lettenmaier (2009a), Use of satellite data to assess the impacts of irrigation withdrawals on Upper Klamath Lake, Oregon, *Hydrol. Earth Syst. Sci.*, 13(5), 617–627, doi:10.5194/hessd-6-1261-2009.
- Tang, Q., S. Peterson, R. H. Cuenca, Y. Hagimoto, and D. P. Lettenmaier (2009b), Satellite-based near-real-time estimation of irrigated crop water consumption, *J. Geophys. Res.*, 114, D05114, doi:10.1029/2008JD010854.
- Tang, Q., H. Gao, P. Yeh, T. Oki, F. Su, and D. P. Lettenmaier (2010), Dynamics of terrestrial water storage change from satellite and surface observations and modeling, *J. Hydrometeorol.*, 11(1), 156–170, doi:10.1175/2009JHM1152.1.
- Thenkabail, P. S., et al. (2009), Global irrigated area map (GIAM), derived from remote sensing for the end of the last millennium, *Int. J. Remote Sens.*, 30(14), 3679–3733, doi:10.1080/01431160802698919.
- Tilman, D., C. Balzer, J. Hill, and B. L. Befort (2011), Global food demand and the sustainable intensification of agriculture, *Proc. Natl. Acad. Sci. U. S. A.*, 108(50), 20,260–20,264, doi:10.1073/pnas.1116437108.
- Voisin, N., H. Li, D. Ward, M. Huang, M. Wigmosta, and L. R. Leung (2013), On an improved sub-regional water resources management representation for integration into earth system models, *Hydrol. Earth Syst. Sci. Discuss.*, 10, 3501–3540, doi:10.5194/hessd-10-3501-2013.
- van Vuuren, D. P., L. Batlle Bayer, C. Chuwah, L. Ganzeveld, W. Hazeleger, B. van den Hurk, T. van Noije, B. O'Neill, and B. J. Strengers (2012), A comprehensive view on climate change: Coupling of Earth system and integrated assessment models, *Environ. Res. Lett.*, 7(2), 024012, doi:10.1088/1748-9326/7/2/024012.
- Xia, Y., M. Ek, H. Wei, and J. Meng (2012), Comparative analysis of relationships between NLDAS-2 forcings and model outputs, *Hydrol. Process.*, 26(3), 467–474, doi:10.1002/hyp.8240.
- Zhu, X., S. Liang, and Y. Pan (2012), Observational evidence of the cooling effect of agricultural irrigation in Jilin, China, *Clim. Change*, 114(3), 799–811, doi:10.1007/s10584-012-0435-3.